# Gradient thresholding algorithm for adaptive colored coded aperture design in compressive spectral imaging

[1] Nelson Diaz , [2] Jorge Bacca, [2] Henry Arguello

[1] *Department of Electrical Engineering, Universidad Industrial de Santander, Bucaramanga, Colombia, 680002*
[2] *Department of Computer Science, Universidad Industrial de Santander, Bucaramanga, Colombia, 680002*

*nelson.diaz@correo.uis.edu.co, jorge.bacca1@correo.uis.edu.co, henarfu@uis.edu.co*

**Abstract:** This paper presents a gradient thresholding algorithm (GTA) to adaptively compute the subsequent colored coded apertures to be used in a compressive spectral imaging sensor yielding to a reconstructed spectral datacube with high image quality.

**OCIS codes:** 110.4234 Multispectral and hyperspectral imaging, 110.1085 Adaptive imaging, 170.1630 Coded aperture imaging

## 1. Introduction

Compressive spectral imaging (CSI) is applied in food safety [1], target detection [2], and classification [3]; it captures projections of an underlying scene, which are the input of recovering algorithms that take advantage of sparsity and high spatial correlation to attain the datacube. Particularly, coded aperture snapshot spectral imaging (CASSI) implements the concepts of CSI [4]. The light in CASSI is spatially modulated by a coded aperture and spectrally by a prism. The light is then integrated into the Focal Plane Array (FPA) forming the compressive measurements. Traditionally, CASSI uses a block-unblock coded aperture which blocks or transmits the spectrum. In contrast, colored-patterned CASSI system (C-CASSI) uses a colored filter array as coded aperture [5]. The advantages of C-CASSI is that the entailed spatio-spectral modulation permits a more flexible coding design. Previous work on C-CASSI has only focused on non-adaptive measurements [5] rather than adaptive measurements. Adaptive means that for $K$ snapshots the compressive measurements $\mathbf{y}^0, \mathbf{y}^1, \cdots, \mathbf{y}^{K-1}$ are sequentially selected and the choice of $\mathbf{y}^{\ell+1}$ depends on the previously gathered measurements $\mathbf{y}^{\ell}$. The fundamental characteristic of adaptive measurements is that they are more outstandingly robust to Gaussian noise than traditional non-adaptive measurements. This work presents a gradient thresholding algorithm (GTA) to adaptively compute colored filter array which will improve the quality of image reconstruction. Results show that the proposed adaptive C-CASSI outperforms the non-adaptive random C-CASSI in up to 2 dBs in terms of PSNR.

## 2. Adaptive colored filter array

The $\ell^{th}$ discretized compressive measurement in C-CASSI can be written as $\mathrm{Y}_{ij}^{\ell} = \sum_{k=0}^{L-1} \mathrm{F}_{i(j-k)k} \mathrm{T}_{i(j-k)k}^{\ell} + \omega_{ij}$, where $\mathrm{Y}_{ij}^{\ell}$ is the intensity in the $(i,j)^{th}$ position, $i = 0, \cdots, N-1$ and $j = 0, \cdots, N+L-1$, $\mathbf{F} \in \mathbb{R}^{N \times N \times L}$ is the underlying scene, where $N$ and $L$ are the spatial resolution and spectral resolution, respectively, and $\mathbf{T} \in \mathbb{R}^{N \times N \times L}$ is a binary three dimensional array modeling the colored filters array, and $\omega_{i,j}$ is the Gaussian noise in the $(i,j)^{th}$ position. The compressive measurements in C-CASSI can be expressed in matrix form as $\mathbf{y}^{\ell} = \mathbf{A}^{\ell}\mathbf{f} + \boldsymbol{\omega}$, where $\mathbf{A}^{\ell}$ stands for the $\ell^{th}$ sensing matrix, $\mathbf{f}$ denotes the vectorization of the underlying datacube $\mathbf{F}$, and $\boldsymbol{\omega}$ is the Gaussian noise. The vectorization of the matrix $\mathbf{F}$ is given by $(\mathrm{f}_k)_j^{\ell} = \boldsymbol{F}_{(j-rN)rk}^{\ell}$, for $j = 0, \cdots, N^2-1$, $k = 0, \cdots, L-1$, $r = \lfloor j/N \rfloor$, where $\ell$ is the shot index $\ell = 0, \cdots, K-1$, and $K$ is the number of snapshots. Equation $\mathbf{y}^{\ell} = \mathbf{A}^{\ell}\mathbf{f} + \boldsymbol{\omega}$ can be rewritten as $\mathbf{y} = \mathbf{A}\mathbf{f}$ where $\mathbf{y} = [(\mathbf{y}^0)^T, \cdots, (\mathbf{y}^{K-1})^T]^T$ and $\mathbf{A} = [(\mathbf{A}^0)^T, \cdots, (\mathbf{A}^{K-1})^T]^T$. Alternatively, $\mathbf{f}$ can be expressed as $\mathbf{f} = \boldsymbol{\Psi}\boldsymbol{\theta}$ where $\boldsymbol{\Psi}$ is an appropriate representation basis and $\boldsymbol{\theta}$ is the vector of sparse coefficients. As a result, $\mathbf{f}$ can be recovered solving the convex optimization problem $\hat{\mathbf{f}} = \boldsymbol{\Psi}(\mathrm{argmin}_{\boldsymbol{\theta}} \|\mathbf{y} - \mathbf{A}\boldsymbol{\Psi}\boldsymbol{\theta}\|_2 + \tau\|\boldsymbol{\theta}\|_1)$. Traditionally, the design of $\mathbf{A}$ is non-adaptive [5]. This paper presents a gradient thresholding algorithm (GTA) to adaptively compute $\mathbf{A}$ in C-CASSI. Particularly, the proposed design increases the transmittance in some areas of $\mathbf{A}$ and decreases in others. Transmittance is the quantity of light transmitted in the system through each filter in C-CASSI. Let $\mathrm{A}_{ij}$ denotes each entry of $\mathbf{A}$, if $\mathrm{A}_{ij} = 1$ the light gets into the system, and, if $\mathrm{A}_{ij} = 0$ the light is filtered out from reaching the Focal Plane Array (FPA).

Figure 1 shows an sketch of the proposed adaptive C-CASSI, when two snapshots are captured. Each shot codes the light spatially and modulates spectrally the coded light. Subsequently, the energy is added in the FPA. The aim of adaptive C-CASSI is to increase the quality of image reconstruction improving the tolerance of the system to Gaussian noise. In order to shape the next projection of the adaptive C-CASSI, GTA algorithm 1 was developed.

Specifically, GTA exploits a low-resolution datacube $\hat{\mathbf{f}}_L$ which provides prior information about the underlying scene $\mathbf{f}$. This method has practical applications since $\hat{\mathbf{f}}_L$ can be obtained with low computational cost. In detail, algorithm 1 receives as an input the first compressive measurement $\mathbf{y}^0$, the initial sensing matrix $\mathbf{A}^0$, and the gradient matrix $\mathbf{B}$. Then in step 3, it computes a low resolution datacube $\hat{\mathbf{f}}_L$. Formally, $\mathbf{f}_L = \mathbf{D}\mathbf{f}$, where $\mathbf{D}$ denotes the decimation matrix and $\mathbf{f}$ identifies the underlying scene. Solving the optimization problem $\hat{\mathbf{f}}_L \leftarrow \mathbf{\Psi}_L(\text{argmin}_{\boldsymbol{\theta}_L}\|\mathbf{y}-\mathbf{A}_L\mathbf{\Psi}_L\boldsymbol{\theta}_L\|_2^2 + \tau\|\boldsymbol{\theta}_L\|_1 + \lambda\|(\mathbf{C}-\mathbf{I})(\mathbf{\Psi}_L\boldsymbol{\theta}_L)\|_2^2)$ s.t $\|\hat{\mathbf{f}}-\mathbf{P}\hat{\mathbf{f}}_L\|_2^2 < \varepsilon$ it obtains the low resolution reconstruction, where $\mathbf{A}_L$ denotes the sensing matrix, $\mathbf{\Psi}_L$ is the representation basis, and $\boldsymbol{\theta}_L$ is the vectorization of a sparse vector for the low resolution reconstruction, $\mathbf{I}$ is the identity matrix, $\mathbf{C}$ is a Gaussian filter to promote smoothness, $\tau$, $\lambda$ are regularization constants and $\mathbf{P}(.)$ is a interpolator of a low resolution datacube. In step 4, the interpolation of a low resolution datacube $\hat{\mathbf{f}}_L$ is computed attaining a high-resolution datacube $\hat{\mathbf{f}}_H$. In step 5, the gradient computation of the high-resolution datacube is given by $\mathbf{g} \leftarrow \mathbf{B}^2\hat{\mathbf{f}}_H$, where $\mathbf{g} \in \mathbb{R}^{N^2\cdot L}$, and $\mathbf{B} \in \mathbb{R}^{N^2\cdot L \times N^2\cdot L}$ is the gradient matrix defined by:

$$\mathbf{B} = \begin{pmatrix} -1 & 1 & 0 & \cdots & 0 & 0 & 0 \\ -0.5 & 0 & 0.5 & \cdots & 0 & 0 & 0 \\ 0 & -0.5 & 0 & \cdots & 0 & 0 & 0 \\ \vdots & \vdots & \vdots & \ddots & \vdots & \vdots & \vdots \\ 0 & 0 & 0 & \ddots & 0 & 0.5 & 0 \\ 0 & 0 & 0 & \cdots & -0.5 & 0 & 0.5 \\ 0 & 0 & 0 & \cdots & 0 & -1 & 1 \end{pmatrix} \otimes \text{diag}(\mathbf{v}), \tag{1}$$

where $\mathbf{v}$ is an all ones vector and $diag(\mathbf{v}) \in \mathbb{R}^{N^2\times N^2}$ is a diagonal matrix whose entries are the elements of $\mathbf{v}$. Then in step 6, the thresholding of the gradient is performed according to the logical operation $\mathbf{q} \leftarrow (\mathbf{g} \preceq \mathbf{0})$, where $\preceq$ is the element-wise inequality, $\mathbf{g}$ is the computed gradient, and $\mathbf{0}$ is an all zero vector. The thresholding $(\mathbf{g} \preceq \mathbf{0})$ splits the spectral signature in concave upward and concave downward. In general, the purpose of the thresholding is to sample at higher transmittance the concave downward regions than the concave upward regions. In step 7, the adaptive colored filter array is computed according to $\mathbf{t} \leftarrow \mathbf{q}\odot\mathbf{t}_d + (\mathbf{1}-\mathbf{q})\odot\mathbf{t}_u$, where $\mathbf{t} \in \mathbb{R}^{N^2\cdot L}$, $\mathbf{t}_d \in \mathbb{R}^{N^2\cdot L}$ has a Bernoulli distribution $\mathbf{t}_d \sim \text{Ber}(d = 2/(\ell+1))$ and $\mathbf{t}_u \in \mathbb{R}^{N^2\cdot L}$ has a Bernoulli distribution $\mathbf{t}_u \sim \text{Ber}(u = 1/\ell)$. The vector $\mathbf{t}_d$ increases the transmittance in concave downward spectral regions and $\mathbf{t}_u$ decreases the transmittance in concave upward spectral regions. The resulting designed colored filter array $\mathbf{t}$, senses with higher transmittance the concave downward spectral regions, than the concave upward spectral regions. For that reason the transmittance $d$ is larger than $u$. In step 10, the vector $t_j^\ell$ is rearranged at the 2D $k^{th}$ plane according to $(\mathbf{t}_k^\ell)_l \leftarrow t_j^\ell$. Afterwards, in step 13, the colored filter array $\mathbf{t}^\ell$ is stacked in the sensing matrix $\mathbf{A}^\ell$ according to $(\mathbf{a}_i)_j \leftarrow (\mathbf{t}_{k_j}^{\ell_i})_{i-\ell_i v-k_j N}$, where $i = 0,\ldots,KV-1$, $V = N+L-1$, $k_j = \lfloor j/N^2 \rfloor$, $\ell_i = \lfloor i/V \rfloor$, $\ell_i \in \{0,\ldots,K-1\}$, and $N' = N^2 - N$. In step 16, the adaptive snapshot is captured as $\mathbf{y}^{\ell+1} \leftarrow \mathbf{A}^{\ell+1}\mathbf{f}$. In step 17, the output of algorithm 1 is the approximation $\hat{\mathbf{f}}$ to $\mathbf{f}$.

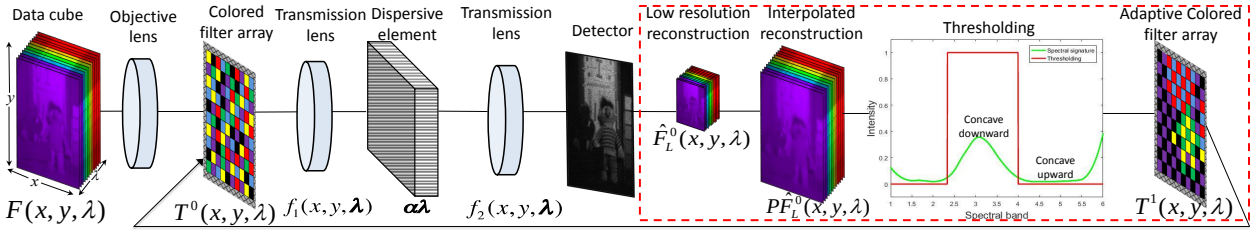


Figure 1: Sketch of adaptive C-CASSI. The figure depicts two snapshots of C-CASSI. The second colored filtered is designed by the GTA, which input is the interpolated datacube $\mathbf{P}\hat{\mathbf{F}}_L$. The dashed line box denotes the proposed adaptive computational process.

## 3. Experiments and results

To assess the capabilities of the adaptive C-CASSI, a comparison with non-adaptive C-CASSI is performed. A critical parameter in the simulation is the transmittance. The transmittance in non-adaptive C-CASSI is traditionally set to 0.5. In adaptive C-CASSI the transmittance is $d = 2/(\ell+1)$ in the concave downward spectral regions, and $u = 1/\ell$ in the concave upward regions. The interpolator $\mathbf{P}$ is a bilinear interpolator. The reconstruction algorithm used is the Gradient Projection for Sparse Reconstruction (GPSR) algorithm [6]. The evaluated spectral image has $N = 512$ pixels of spatial resolution and $L = 12$ spectral bands. Figure 2a shows the original first spectral band, the reconstruction of non-adaptive, and the adaptive C-CASSI. The figure 2b shows the quality of image reconstruction against the number of snapshots with Gaussian noise with SNR of 10 dB, 20 dB and 30 dB. The dashed line represents the non-adaptive C-

**Algorithm 1** GTA gradient thresholding algorithm.

**Require:** $\mathbf{y}^0$, $\mathbf{A}^0$, $\mathbf{B}$
**Ensure:** $\hat{\mathbf{f}}$
**function** GTA($\mathbf{y}^0$, $\mathbf{A}^0$, $\mathbf{B}$)
  **for** $\ell \leftarrow 0, K-1$ **do**
    $\hat{\mathbf{f}}_L^\ell \leftarrow \mathbf{\Psi}_L(\text{argmin}_{\boldsymbol{\theta}_L} \|\mathbf{y} - \mathbf{A}_L\mathbf{\Psi}_L\boldsymbol{\theta}_L\|_2^2 + \tau\|\boldsymbol{\theta}_L\|_1 + \lambda\|(\mathbf{C}-\mathbf{I})(\mathbf{\Psi}_L\boldsymbol{\theta}_L)\|_2^2)$ ▷ Low-resolution
    $\hat{\mathbf{f}}_H^\ell \leftarrow \mathbf{P}\hat{\mathbf{f}}_L^\ell$ ▷ Interpolation
    $\mathbf{g}^\ell \leftarrow \mathbf{B}^2\hat{\mathbf{f}}_H^\ell$ ▷ Compute gradient
    $\mathbf{q}^\ell \leftarrow (\mathbf{g}^\ell \preceq \mathbf{0})$ ▷ Thresholding
    $\mathbf{t}^\ell \leftarrow \mathbf{q}^\ell \odot \mathbf{t}_d^\ell + (\mathbf{1}-\mathbf{q}^\ell) \odot \mathbf{t}_u^\ell$, ▷ Transmittance
  **for** $j \leftarrow 0, N^2L-1$ **do**
    $k = \lfloor j/N^2 \rfloor$, $l = j \mod N^2$
    $(\mathbf{t}_k^\ell)_l \leftarrow t_j^\ell$ ▷ Rearrange $\mathbf{t}$
  **for** $i \leftarrow 0, KV-1$ **do**
    **if** $i - \ell_i V = j - k_j N'$ **then**
      $(\mathbf{a}_i)_j \leftarrow (\mathbf{t}_{k_j}^{\ell_i})_{i-\ell_i v - k_j N}$ ▷ Compute $\mathbf{A}$
    **else**
      $(\mathbf{a}_i)_j \leftarrow 0$
  $\mathbf{y}^{\ell+1} \leftarrow \mathbf{A}^{\ell+1}\mathbf{f}$ ▷ Next snapshot
**return** $\hat{\mathbf{f}} \leftarrow \mathbf{\Psi}(\text{argmin}_{\boldsymbol{\theta}} \|\mathbf{y} - \mathbf{A}\mathbf{\Psi}\boldsymbol{\theta}\|_2 + \tau\|\boldsymbol{\theta}\|_1)$

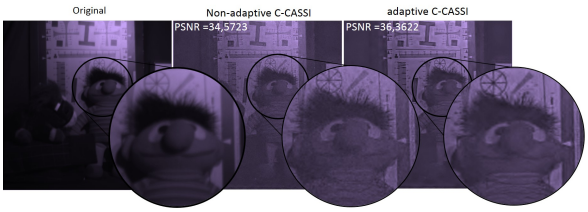


(a) The figure depicts a comparison of the first spectral band between the original, the non-adaptive C-CASSI and adaptive C-CASSI.

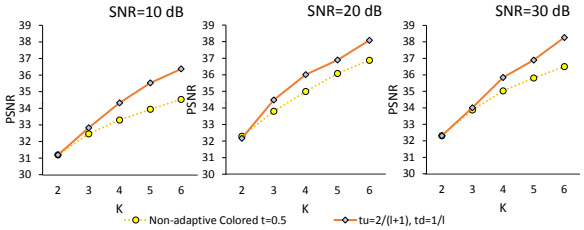


(b) The figure shows the quality of image reconstruction against the number of snapshots, the simulations include tests with Gaussian noise with SNR=10 dB, 20 dB and 30 dB.

Figure 2: The results show that the proposed method outperforms in up to 2 dB the traditional method.

CASSI and the solid line represents the adaptive C-CASSI. The proposed method outperforms the traditional method in up to 2 dB when SNR = 10 dB. The most remarkable result from the data is that adaptive C-CASSI is significantly more robust in presence of Gaussian noise than non-adaptive C-CASSI. The benefits in terms of suitable performance to Gaussian noise and improvements in the quality of image reconstruction far outweigh the disadvantage with regards to the computational cost to compute a low-resolution scene $\hat{\mathbf{f}}_L$. In addition, the proposed method represents an useful alternative to deal with Gaussian noise in real scenarios.

## 4. Conclusions

An adaptive C-CASSI system was proposed as an alternative to non-adaptive C-CASSI with the advantage of improved quality of image reconstruction which deal better with the Gaussian noise. The proposed method outperforms the traditional method in up to 2 dB.

## References

1. Z. Du, M. K. Jeong and S. G. Kong, "Band Selection of Hyperspectral Images for Automatic Detection of Poultry Skin Tumors," in *IEEE Transactions on Automation Science and Engineering*, Vol. 4, no. 3, pp. 332-339, July 2007.
2. A. Alarcon-Ramirez, M. R. Rwebangira, M. F. Chouikha and V. Manian, "A New Methodology Based on Level Sets for Target Detection in Hyperspectral Images," in *IEEE Transactions on Geoscience and Remote Sensing*, vol. 54, no. 9, pp. 5385-5396, Sept. 2016.
3. Q. Lv, X. Niu, Y. Dou, J. Xu, and Y. Lei, "Classification of Hyperspectral Remote Sensing Image Using Hierarchical Local-Receptive-Field-Based Extreme Learning Machine," in *IEEE Geoscience and Remote Sensing Letters*, vol. 13, no. 3, pp. 434-438, March 2016.
4. A. Wagadarikar, R. John, R. Willett, and D. Brady, "Single disperser design for coded aperture snapshot spectral imaging," in *Optical Society of America*, vol. 47, pp. B44–B51, 2008.
5. H. Arguello and G. R. Arce, "Colored Coded Aperture Design by Concentration of Measure in Compressive Spectral Imaging," in *IEEE Transactions on Image Processing*, vol. 23, no. 4, pp. 1896-1908, April 2014.
6. M. A. T. Figueiredo, R. D. Nowak and S. J. Wright, "Gradient Projection for Sparse Reconstruction: Application to Compressed Sensing and Other Inverse Problems," in *IEEE Journal of Selected Topics in Signal Processing*, vol. 1, no. 4, pp. 586-597, Dec. 2007.